ACS APPLIED MATERIALS & INTERFACES

Letter

www.acsami.org

Surface Modification of Silver Nanowires for Morphology and Processing Control in Composite Transparent Electrodes

Zhiming Liang[†] and Kenneth R. Graham*[,†]

[†]Department of Chemistry, University of Kentucky, Lexington, Kentucky 40506, United States

Supporting Information

ABSTRACT: Silver nanowires are attractive components for a number of materials and applications, including silver nanowire (AgNW)−polymer composites, electrically conductive coatings, and transparent electrodes. In this manuscript, the ability of thiols with hydrophobic to ionic end groups to bind to AgNW surfaces is investigated, followed by how the polarity of the surface modifying thiol influences the morphological and electrical properties of both AgNW/PEDOT:PSS blend films and pure AgNW networks. Utilizing surface modification of AgNWs with sodium 3-mercapto-1-propanesulfonate (MPS), morphologically homogeneous AgNW/PEDOT:PSS thin films with an order of magnitude lower sheet resistance at similar transmittance values than unmodified AgNWs are obtained with a one-step processing method. Brief optimization of MPS-AgNW/PEDOT:PSS blends yields a sheet resistance of 22.6 Ω/□ at 81.4% transmittance.

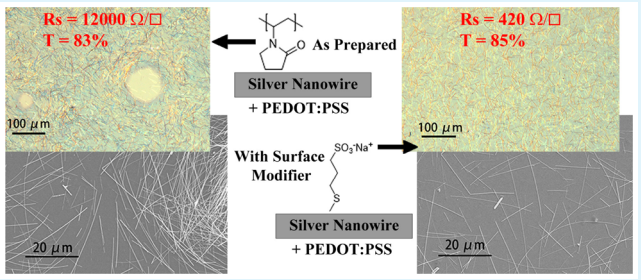

KEYWORDS: *surface modification, silver nanowire, transparent electrode, polymer-nanowire composite, morphology*

Transparent electrodes are required in a number of optoelectronic devices, such as light emitting displays, touch screens, and solar cells.[1,2] For these applications the electrodes should be highly transparent to visible light with a low sheet resistance (R_S). Indium tin oxide (ITO), likely the most widely used material for transparent electrodes, meets these requirements with >90% transmittance at 550 nm and a R_S of 10 Ω/□ on glass.[3] However, there are multiple disadvantages of ITO for use in the upcoming generation of lower cost, flexible, solution-processed electronics; namely, ITO has poor mechanical flexibility, cannot be solution-processed, and includes indium, which is expensive and in limited supply.[2,3] Thus, alternative materials that will enable large-scale, rapid, and inexpensive solution-processed devices, as well as flexible electronics, are being widely explored.[2,4,5] Attractive alternatives to ITO include carbon nanotube films (R_S = 60 Ω/□ at T = 90.9%),[6−8] graphene (R_S = 21.26 Ω/□ at T = 88%),[9] and metal nanowires such as Ag (R_S = 13 Ω/□ at T = 85%, R_S = 20 Ω/□ at T = 93%)[10,11] and Cu (R_S = 24 Ω/□ at T = 88%, R_S = 100 Ω/□ at T = 92−93%).[12,13] Higher performance metrics for AgNWs (R_S = 8.5Ω/□ at T = 90%) and CuNWs (R_s = 11.2 Ω/□ at T = 91%) are also possible using an electrospinning fabrication method, though the wire diameters are significantly larger at around 500 nm.[14] Compared with carbon materials, metal nanowire films typically demonstrate lower R_S at comparable transmittance. Of the metal NWs, Ag is more widely studied owing to its higher oxidative stability over Cu, with Ag NW networks maintaining high conductivity over 2.5 years under ambient conditions,[15] and more neutral color as opposed to the orange hue of CuNWs.

Commonly, AgNWs are incorporated into composites with polymers to improve both mechanical and electrical properties. The conductive polymer blend poly(3,4-ethylenedioxythiophene):polystyrenesulfonate (PEDOT:PSS) is a common choice in AgNW-polymer composites for transparent electrodes, where PEDOT:PSS serves multiple roles including filling the voids between AgNWs, work function modification, and planarization. Various methods have been reported to fabricate transparent AgNW/PEDOT:PSS electrodes; including subsequent spray deposition of AgNWs and PEDOT:PSS, spray deposition of AgNWs followed by embedding the AgNW network into PEDOT:PSS,[16] and subsequent coating of AgNWs, poly(vinyl alcohol), and PEDOT:PSS.[17] However, all these methods are either multistep processes or yield films with large surface roughness. The need for multistep processing rests in part with the difficulty in dispersing both polymers and AgNWs in the same solvent, achieving good electrical contact between AgNWs, and creating morphologically homogeneous films. To the best of our knowledge, only one report currently exists of a one-step processing method for AgNW/PEDOT:PSS films; however, in that work it is not clear if the films are homogeneous over a large scale, and if so, it is not clear how this was achieved.[18]

In the work reported herein, we investigate if thiols with hydrophobic to ionic end groups will effectively modify AgNW surfaces, and how the polarity of the surface modifier influences

Received: July 19, 2015
Accepted: September 21, 2015
Published: September 21, 2015

DOI: 10.1021/acsami.5b06489
ACS Appl. Mater. Interfaces 2015, 7, 21652−21656

the morphological and electrical properties of both AgNW/PEDOT:PSS blends and pure AgNW networks. It will be shown that surface modification with appropriate thiols allows for compatibility with polymers, such as PEDOT:PSS, and solvents to be controllably adjusted while simultaneously reducing wire-to-wire junction resistance. Utilizing this surface modification strategy, a one-step processing method is demonstrated for the fabrication of morphologically homogeneous AgNW/PEDOT:PSS composite films. Surprisingly, there are few previous reports of AgNW modification with thiols,[19−21] despite the facile modification process and versatility it provides. Herein, it is demonstrated that AgNWs can be readily modified with thiols ranging from ionic to hydrophobic, with the thiols displacing the polyvinylpyrrolidone (PVP) previously present on the AgNW surface. Surface modification not only allows the compatibility with polymers and solvents to be tuned,[21,22] but it can also significantly decrease wire-to-wire junction resistances. As will be demonstrated, this combination of improved compatibility and minimized junction resistance leads to uniform AgNW/PEDOT:PSS films with high transmittance and low R_S.

To probe whether as-prepared PVP coated AgNWs can be modified with thiols, X-ray photoelectron spectroscopy (XPS) is used to compare sulfur binding energies between pure sodium 3-mercapto-1-propanesulfonate (MPS) and MPS modified AgNWs (MPS-AgNWs). As shown in Figure 1, sulfur

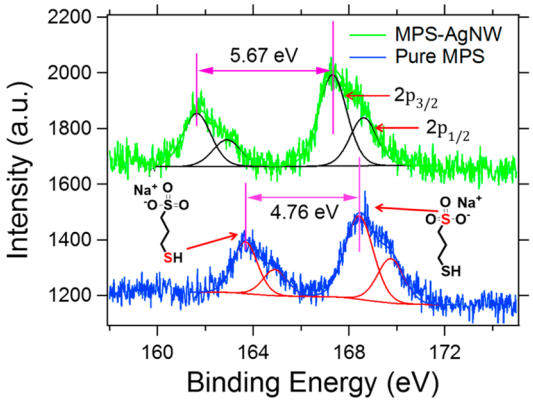

Figure 1. XPS spectra of pristine MPS S 2p and MPS-AgNWs S 2p.

is clearly present in the XPS spectrum of the MPS-AgNW sample, indicating that MPS remains adsorbed on the AgNW surfaces following rinsing in ethanol and deionized water. Analysis of S peak positions in the XPS spectra further support MPS binding to the AgNWs. The XPS spectrum of pure MPS shows $2p_{3/2}$ binding energies of 163.69 and 168.45 eV for mercapto and sulfonate sulfurs, respectively, which is a difference of 4.76 eV. For MPS-AgNWs, the mercapto sulfur $2p_{3/2}$ peak is shifted to lower binding energy by 2.05 at 161.64 eV, whereas the sulfonate sulfur $2p_{3/2}$ binding energy is shifted by only 1.14 to 167.31 eV, a difference of 5.67 eV between sulfur peaks as highlighted in Figure 1. This larger shift in the binding energy of the mercapto sulfur in the MPS-AgNW sample strongly supports that this sulfur is binding with the AgNW surface. As expected, the same trend exists for the S 2s peaks as shown in Figure S1.

The synthesis of AgNWs involves the use of PVP to stabilize and promote one-dimensional growth, resulting in PVP-coated AgNWs.[23] To determine if this PVP is displaced through the surface modification of AgNWs, the nitrogen 1s peak in the XPS spectra is examined. Figure S1 shows a strong N 1s peak at 400.29 eV originating from the N atom in the PVP repeat unit. In contrast, MPS modified AgNWs display no evidence of this N 1s peak. This data indicates that MPS displaces PVP on the AgNW surface. Importantly, this displacement of PVP lowers the wire-to-wire junction resistance, as will be highlighted later in the manuscript.

Silver nanowires were also modified with decanethiol (DT) and mercaptoethanol (MEtOH), and as expected DT-AgNWs display distinctly different dispersibility than MEtOH- and MPS-AgNWs. For example, DT-AgNWs disperse well in ethanol and are completely aggregated in deionized water (Figure S2). By contrast, MPS-AgNW dispersions are more stable in water than in ethanol (Figure S2). MEtOH-AgNWs are also well-dispersed in water and ethanol. These data confirm that AgNW dispersibility can be readily tuned through thiol modification. Control over dispersibility is particularly relevant to the development of completely solution-processed electronics, where orthogonal solvents are generally necessary for processing multilayer devices.

The effects of surface modifier on the morphology of AgNW/PEDOT:PSS blend films is examined through optical microscopy and scanning electron microscopy (SEM), where for this comparison all AgNWs are from Blue Nano (BN). Silver NW/PEDOT:PSS blends with varying surface modifiers are compared at AgNW to PEDOT:PSS weight ratios of 1:9, 2:8, and 4:6, with Figure 2 showing AgNW/PEDOT:PSS weight ratios of 2:8. These images, as well as those included in Figures S3 and S4, reveal that MPS- and MEtOH-AgNW/PEDOT:PSS films are uniform with AgNW weight ratios up to 4:6. On the other hand, DT-AgNW/PEDOT:PSS films are inhomogeneous with large aggregated regions appearing even at the lower 1:9 DT-AgNW/PEDOT:PSS ratio. Unmodified-AgNW/PEDOT:PSS films are more uniform than the DT-AgNW blends, though these films are not morphologically homogeneous as larger-scale defects appear at AgNW/PEDOT:PSS wt. ratios at and above 1:9 (Figure S3).

The trend in film quality with MPS-AgNWs and DT-AgNWs forming the most and least homogeneous films with PEDOT:PSS, respectively, are predicted from considerations of basic electrostatic interactions. Here the anionic sulfonate group of MPS interacts strongly with the cationic PEDOT, with this strong ionic interaction resulting in homogeneous MPS-AgNW/PEDOT:PSS films. The hydrophilic and more polar MEtOH modified silver nanowires will also interact favorably with the aqueous solvent and PEDOT:PSS, thus also yielding homogeneous films. The behavior of PVP coated NWs is not readily explained, as PVP is also water-soluble and would be expected to have similar interactions with PEDOT:PSS as those of MEtOH. Experimental evidence suggests the O and N atoms in PVP interact more strongly with the AgNW surface,[24−26] which leaves the less polar alkyl groups more exposed to interact with PEDOT:PSS. These alkyl group interactions with PEDOT:PSS will be less favorable than the alcohol−PEDOT:PSS interactions and may explain the nonuniform morphologies of the UM-AgNW/PEDOT:PSS blends, though extensive further studies would be necessary to offer a definitive explanation. The least polar and hydrophobic DT leads to unfavorable interactions with both PEDOT:PSS and the aqueous solvent, resulting in significant DT-AgNW aggregation. Thus, as the images Figure 2 show, film morphologies vary

DOI: 10.1021/acsami.5b06489
ACS Appl. Mater. Interfaces 2015, 7, 21652−21656

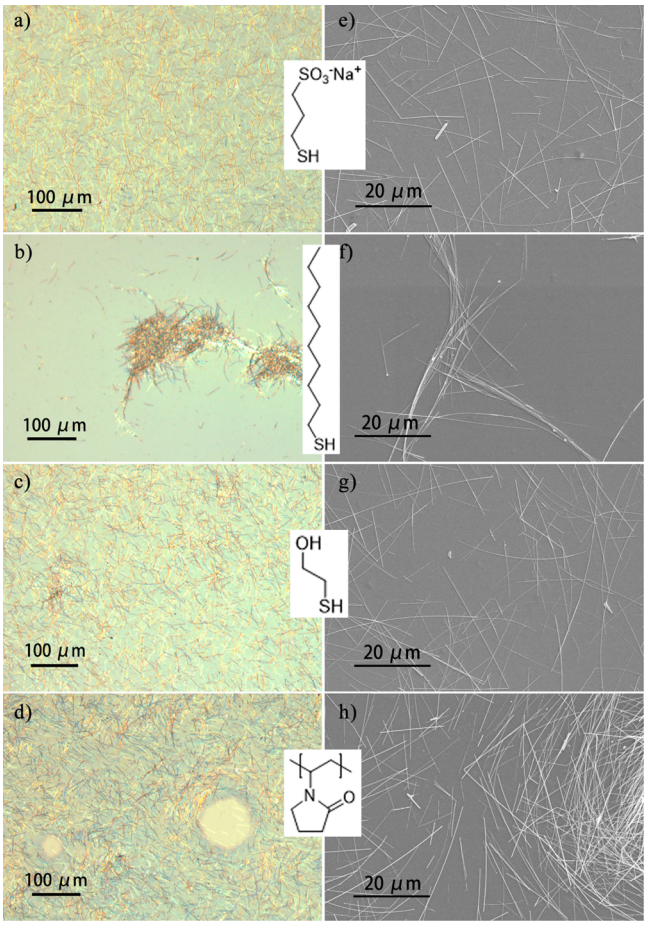

Figure 2. Optical (left) and SEM (right) images of AgNW/PEDOT:PSS blends at 2:8 wt. ratios: (a, e) MPS-AgNWs; (b, f) DT-AgNWs; (c, g)MEtOH-AgNWs; and (d, h) UM−AgNWs.

based on the interaction of the surface modifier with both the aqueous solvent and PEDOT:PSS.

Transmittance (T) vs sheet resistance (R_S) data are shown for the AgNW/PEDOT:PSS blend films in Figure 3. Each

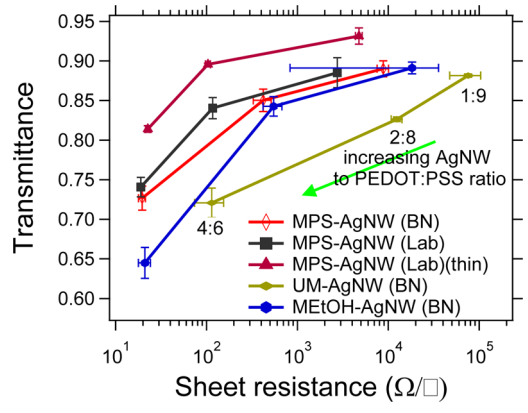

Figure 3. Sheet resistance vs transmittance at 550 nm of AgNW/PEDOT:PSS films at weight ratios of 1:9, 2:8, and 4:6 (PEDOT:PSS concentration is 1.1 wt % prior to blending with AgNWs), with the exception of MPS-AgNW(Lab) (thin), for which weight ratios are 1:6, 2:5.3, and 1:1 (PEDOT:PSS was diluted from 1.1 to 0.73 wt % prior to blending with AgNWs). Transmittance values are of AgNW films only, i.e., an uncoated glass slide is treated as 1.0 T.

series, whereby the only parameter changed is the AgNW/PEDOT:PSS ratio, shows a 1.5 to 3 order of magnitude decrease in R_S as the AgNW ratio is increased from 1:9 to 4:6. Accompanying this drop in R_S is a decrease of 0.12 to 0.24 in T. This decrease in R_S and T with increasing AgNW concentration is attributed primarily to the contribution of the AgNWs, though the PEDOT:PSS film thickness also increases with AgNW concentration (Table S1). Surprisingly, at similar transmittance values, MPS- and MEtOH-AgNW/PEDOT:PSS films display approximately an order of magnitude lower R_S than the UM-AgNW/PEDOT:PSS films. As will be discussed, this trend is likely attributed to the higher wire-to-wire junction resistance of the PVP-coated AgNWs. Thus, modification of the AgNWs with MPS or MEtOH has two complementary effects that include uniform film morphologies and lower R_S at comparable T.

Original experiments with MPS-AgNW/PEDOT:PSS blends containing BN AgNWs yielded respectable values of 20 Ω /□ at 73% T, though multiple optimizations are possible to improve these performance metrics. For example, the electronic properties of silver nanowire films are greatly affected by lengths and diameters of the AgNWs, with larger L/D ratios resulting in decreased R_S at similar transmittance values.[27−29] Original experiments were carried out with AgNWs purchased from Blue Nano (BN), with a diameter observed through SEM of 118 ± 34 nm and length of 28.7 ± 14.7 μm as shown in Figure S8. In an effort to improve performance metrics, we synthesized AgNWs in our laboratory (Lab) based on the procedure reported by Ran et al.[29] Our synthesis yielded AgNWs with a diameter of 59 ± 11 nm and lengths of 37 ± 21 μm (Figure S9). As shown in Figure 3, films utilizing MPS-AgNWs(Lab) display slightly better performance than MPS-AgNWs(BN). Taking AgNWs at weight ratios equal to 4:6 for instance, MPS-AgNW(BN) has a T = 72.7 ± 1.5% at R_S = 19.6 ± 1.7 Ω/□, whereas MPS-AgNW(Lab) has a T = 74.1 ± 1.2% at R_S = 18.9 ± 1.7 Ω/□.

The transmittance may be further optimized through reducing the overall film thickness and further increasing the relative AgNW concentration. Here PEDOT:PSS was diluted from 1.1 to 0.73 wt %, resulting in thinner films with MPS-AgNW/PEDOT:PSS wt. ratios of 1:6, 2:5.3, and 1:1 (Table S1). Figure 3 displays higher performance for these MPS-AgNW(Lab)/PEDOT:PSS(thin) blends. At a weight ratio of 1:1, these thinner films (thickness of 110 ± 9 nm vs 160 ± 7 nm for nondilute blends) display R_S = 22.6 ± 1.2 Ω/□ and T = 81.4 ± 0.4% with similar homogeneous film morphologies, as shown in Figures S5−S7. Although detailed stability studies were not performed, we found that the R_S of 4:6 MEtOH- and MPS-AgNW/PEDOT:PSS films increased by 25% (MPS) to 50% (MEtOH) over a period of 6 months storage in ambient conditions, whereas the 2:8 blends with higher initial R_S increased by more than an order of magnitude for all AgNW/PEDOT:PSS blends. This trend is consistent with previous literature and is likely the result of PEDOT:PSS instability in air as opposed to degradation of the AgNWs.[15]

As evident in Figure 3, UM-AgNW(BN)/PEDOT:PSS blends show approximately an order of magnitude higher R_S than MPS or MEtOH modified AgNW(BN) blends at similar T. To determine if the lower R_S of MPS-and MEtOH-AgNW/PEDOT:PSS blends is due to increased wire-to-wire charge transfer rates (lower junction resistance) or increased charge transfer rates between AgNWs and PEDOT:PSS, AgNW films are compared in the absence of any polymer host and in the

DOI: 10.1021/acsami.5b06489
ACS Appl. Mater. Interfaces 2015, 7, 21652−21656

presence of an insulating polymer host in place of PEDOT:PSS. If increased AgNW-to-AgNW charge transfer rates are responsible for the lower R_S of MEtOH-AgNW/PEDOT:PSS films, as opposed to improved charge transfer between AgNWs and PEDOT:PSS, then the AgNW films in the absence of PEDOT:PSS should show a similar trend as those with PEDOT:PSS. As shown in Figure 4, films prepared in the absence of a polymer host indeed show a similar R_S trend as those with PEDOT:PSS, with MEtOH-AgNW films displaying an R_S of 22.3 ± 2.4 Ω/□ vs 100 ± 34 Ω/□ for UM-AgNWs. As shown in Figure S10, these films show comparable absorbance values at the AgNW absorbance peak of 355 nm (0.11 ± 0.01 and 0.14 ± 0.01 for MEtOH-AgNWs and UM-AgNWs, respectively) and similar transmittance values at 550 nm (83.7 and 85.5% T for MEtOH-AgNWs and UM-AgNWs, respectively), with the UM-AgNWs even displaying a slightly higher absorbance and still a higher R_S. Varying degrees of AgNW aggregation may be suggested as a potential explanation, but as shown in Figure S13, the AgNW network morphologies are nearly identical. These images in Figure S13 correspond with the data set shown in Figure S11, which is from an identical experiment as presented in Figure 4, but repeated approximately 6 months after the original experiments. Both experiments show a similar trend, thereby further verifying the reproducibility of the data. Furthermore, after annealing at 200 and 250 °C, at which point junction resistance is nearly eliminated as the nanowires fuse together, the R_S values converge to around 10 Ω/□. This comparable R_S after high temperature annealing, combined with nearly identical AgNW network morphologies, strongly supports that the MEtOH-AgNW films (both in pure form and blends with PEDOT:PSS) have lower R_S values due to lower AgNW-to-AgNW junction resistance than UM-AgNWs.

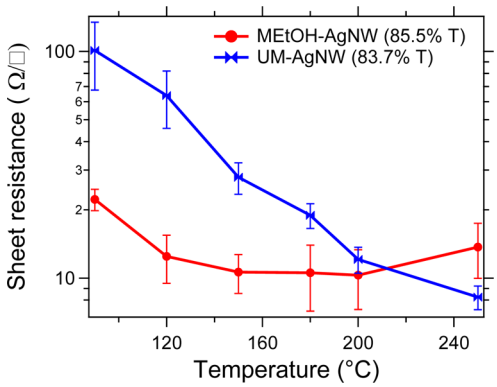

Figure 4. Temperature vs Sheet resistance of MEtOH-AgNW and UM-AgNW. Transmittance is given at 550 nm.

Further verification that the AgNW-to-AgNW junction resistance is lower in MEtOH-AgNWs than in UM-AgNWs is demonstrated by comparing the effects of an insulating polymer matrix. Here, the system is morphologically as similar as possible to the PEDOT:PSS blend, only the polymer host is the nonconductive polymer PVP. Mercaptoethanol-AgNW(BN)/PVP and UM-AgNW(BN)/PVP (Film absorbance at AgNW λ_{max}(355 nm)= 0.06 ± 0.01, 7:3 AgNW/PVP weight ratio) blend films' sheet resistance and transmittance are examined, and similar to the PEDOT:PSS blends the UM-AgNW/PVP film has approximately an order of magnitude higher R_S than MEtOH-AgNW/PVP films after annealing at 25 °C, 120 °C, and 140 °C (Figure S12). Because of the insulating polymer host, the absolute R_S values of both films are approximately an order of magnitude higher than with PEDOT:PSS as the host polymer. All films have similar morphology (Figure S14), thus further supporting that displacement of PVP with MEtOH on the AgNW surface lowers the AgNW-to-AgNW junction resistance.

In summary, surface modification of AgNWs provides a means of controllably altering dispersibility, compatibility with various polymers, and minimizing wire-to-wire junction resistance. Through blending MPS-AgNWs with PEDOT:PSS, uniform films that can be utilized as transparent electrodes for electronic devices were formed with a one-step solution processing method. The facile surface modification of AgNWs with thiols opens up a variety of promising future uses. These could include controllably altering dispersibility of AgNWs for utilization in multistep solution-processed devices where orthogonal solvents are needed, and increasing compatibility with various polymers to create electrically conductive polymer films with mechanical properties such as flexibility or strechability.

■ ASSOCIATED CONTENT

Supporting Information

The Supporting Information is available free of charge on the ACS Publications website at DOI: 10.1021/acsami.5b06489.

Experimental methods, characterization, and additional figures and tables
(PDF)

■ AUTHOR INFORMATION

Corresponding Author

*E-mail: Kenneth.graham@uky.edu.

Author Contributions

The manuscript was written through contributions of all authors. All authors have given approval to the final version of the manuscript.

Funding

The authors acknowledge the University of Kentucky for providing start-up funds.

Notes

The authors declare no competing financial interest.

■ REFERENCES

(1) Bonaccorso, F.; Sun, Z.; Hasan, T.; Ferrari, A. C. Graphene Photonics and Optoelectronics. *Nat. Photonics* **2010**, *4* (9), 611−622.
(2) Ye, S.; Rathmell, A. R.; Chen, Z.; Stewart, I. E.; Wiley, B. J. Metal Nanowire Networks: The Next Generation of Transparent Conductors. *Adv. Mater.* **2014**, *26* (39), 6670−6687.
(3) Cairns, D. R.; Witte, R. P.; Sparacin, D. K.; Sachsman, S. M.; Paine, D. C.; Crawford, G. P.; Newton, R. R. Strain-Dependent Electrical Resistance of Tin-Doped Indium Oxide on Polymer Substrates. *Appl. Phys. Lett.* **2000**, *76* (11), 1425−1427.
(4) Langley, D.; Giusti, G.; Mayousse, C.; Celle, C.; Bellet, D.; Simonato, J. P. Flexible Transparent Conductive Materials Based on Silver Nanowire Networks: A Review. *Nanotechnology* **2013**, *24*, 452001.
(5) Li, L.; Yu, Z. B.; Hu, W. L.; Chang, C. H.; Chen, Q.; Pei, Q. B. Efficient Flexible Phosphorescent Polymer Light-Emitting Diodes Based on Silver Nanowire-Polymer Composite Electrode. *Adv. Mater.* **2011**, *23* (46), 5563−5567.

DOI: 10.1021/acsami.5b06489
ACS Appl. Mater. Interfaces 2015, 7, 21652−21656

(6) Hecht, D. S.; Heintz, A. M.; Lee, R.; Hu, L.; Moore, B.; Cucksey, C.; Risser, S. High Conductivity Transparent Carbon Nanotube Films Deposited from Superacid. *Nanotechnology* **2011**, *22*, 169501.
(7) Blackburn, J. L.; Barnes, T. M.; Beard, M. C.; Kim, Y. H.; Tenent, R. C.; McDonald, T. J.; To, B.; Coutts, T. J.; Heben, M. J. Transparent Conductive Single-Walled Carbon Nanotube Networks with Precisely Tunable Ratios of Semiconducting and Metallic Nanotubes. *ACS Nano* **2008**, *2* (6), 1266−1274.
(8) Rowell, M. W.; Topinka, M. A.; McGehee, M. D.; Prall, H.-J. r.; Dennler, G.; Sariciftci, N. S.; Hu, L.; Gruner, G. Organic Solar Cells with Carbon Nanotube Network Electrodes. *Appl. Phys. Lett.* **2006**, *88*, 233506.
(9) Ning, J.; Wang, D.; Zhang, C.; Wang, Z.; Tang, S.; Chen, D.; Shi, Y.; Zhang, J.; Hao, Y. Electrical and Optical Properties of Layer-Stacked Graphene Transparent Electrodes Using Self-Supporting Transfer Method. *Synth. Met.* **2015**, *203*, 215−220.
(10) De, S.; Higgins, T. M.; Lyons, P. E.; Doherty, E. M.; Nirmalraj, P. N.; Blau, W. J.; Boland, J. J.; Coleman, J. N. Silver Nanowire Networks as Flexible, Transparent, Conducting Films: Extremely High Dc to Optical Conductivity Ratios. *ACS Nano* **2009**, *3* (7), 1767−1774.
(11) Chang, M. H.; Cho, H. A.; Kim, Y. S.; Lee, E. J.; Kim, Y. J. Thin and Long Silver Nanowires Self-Assembled in Ionic Liquids as a Soft Template: Electrical and Optical Properties. *Nanoscale Res. Lett.* **2014**, *9*, 330.
(12) Ye, S. R.; Rathmell, A. R.; Stewart, I. E.; Ha, Y. C.; Wilson, A. R.; Chen, Z. F.; Wiley, B. J. A Rapid Synthesis of High Aspect Ratio Copper Nanowires for High-Performance Transparent Conducting Films. *Chem. Commun.* **2014**, *50* (20), 2562−2564.
(13) Sachse, C.; Weiss, N.; Gaponik, N.; Muller-Meskamp, L.; Eychmuller, A.; Leo, K. Ito-Free, Small-Molecule Organic Solar Cells on Spray-Coated Copper-Nanowire-Based Transparent Electrodes. *Adv. Energy Mater.* **2014**, *4*, 1300737.
(14) Hsu, P. C.; Kong, D. S.; Wang, S.; Wang, H. T.; Welch, A. J.; Wu, H.; Cui, Y. Electrolessly Deposited Electrospun Metal Nanowire Transparent Electrodes. *J. Am. Chem. Soc.* **2014**, *136* (30), 10593−10596.
(15) Mayousse, C.; Celle, C.; Fraczkiewicz, A.; Simonato, J. P. Stability of Silver Nanowire Based Electrodes under Environmental and Electrical Stresses. *Nanoscale* **2015**, *7* (5), 2107−2115.
(16) Gaynor, W.; Burkhard, G. F.; McGehee, M. D.; Peumans, P. Smooth Nanowire/Polymer Composite Transparent Electrodes. *Adv. Mater.* **2011**, *23* (26), 2905−2910.
(17) Zeng, X. Y.; Zhang, Q. K.; Yu, R. M.; Lu, C. Z. A New Transparent Conductor: Silver Nanowire Film Buried at the Surface of a Transparent Polymer. *Adv. Mater.* **2010**, *22* (40), 4484−4488.
(18) Kim, Y.-S.; Chang, M.-H.; Lee, E.-J.; Ihm, D.-W.; Kim, J.-Y. Improved Electrical Conductivity of Pedot-Based Electrode Films Hybridized with Silver Nanowires. *Synth. Met.* **2014**, *195*, 69−74.
(19) Hsiao, S.-T.; Tien, H.-W.; Liao, W.-H.; Wang, Y.-S.; Li, S.-M.; Mma, C.-C.; Yu, Y.-H.; Chuang, W.-P. A Highly Electrically Conductive Graphene−Silver Nanowire Hybrid Nanomaterial for Transparent Conductive Films. *J. Mater. Chem. C* **2014**, *2* (35), 7284−7291.
(20) Andrew, P.; Ilie, A. Functionalised Silver Nanowire Structures. *J. Phys.: Conf. Ser.* **2007**, *61*, 36−40.
(21) Wu, K. H.; Lu, S. Y. Preferential Partition of Nanowires in Thin Films of Immiscible Polymer Blends. *Macromol. Rapid Commun.* **2006**, *27* (6), 424−429.
(22) Bauer, C. A.; Stellacci, F.; Perry, J. W. Relationship between Structure and Solubility of Thiol-Protected Silver Nanoparticles and Assemblies. *Top. Catal.* **2008**, *47* (1−2), 32−41.
(23) Sun, Y. G.; Gates, B.; Mayers, B.; Xia, Y. N. Crystalline Silver Nanowires by Soft Solution Processing. *Nano Lett.* **2002**, *2* (2), 165−168.
(24) Zhang, Z. T.; Zhao, B.; Hu, L. M. Pvp Protective Mechanism of Ultrafine Silver Powder Synthesized by Chemical Reduction Processes. *J. Solid State Chem.* **1996**, *121* (1), 105−110.
(25) Mdluli, P. S.; Sosibo, N. M.; Revaprasadu, N.; Karamanis, P.; Leszczynski, J. Surface Enhanced Raman Spectroscopy (Sers) and Density Functional Theory (Dft) Study for Understanding the Regioselective Adsorption of Pyrrolidinone on the Surface of Silver and Gold Colloids. *J. Mol. Struct.* **2009**, *935* (1−3), 32−38.
(26) Gao, Y.; Jiang, P.; Liu, D. F.; Yuan, H. J.; Yan, X. Q.; Zhou, Z. P.; Wang, J. X.; Song, L.; Liu, L. F.; Zhou, W. Y.; Wang, G.; Wang, C. Y.; Xie, S. S.; Zhang, J. M.; Shen, A. Y. Evidence for the Monolayer Assembly of Poly(Vinylpyrrolidone) on the Surfaces of Silver Nanowires. *J. Phys. Chem. B* **2004**, *108* (34), 12877−12881.
(27) Jiu, J.; Araki, T.; Wang, J.; Nogi, M.; Sugahara, T.; Nagao, S.; Koga, H.; Suganuma, K.; Nakazawa, E.; Hara, M.; Uchida, H.; Shinozaki, K. Facile Synthesis of Very-Long Silver Nanowires for Transparent Electrodes. *J. Mater. Chem. A* **2014**, *2* (18), 6326−6330.
(28) Lee, J.; Lee, P.; Lee, H.; Lee, D.; Lee, S. S.; Ko, S. H. Very Long Ag Nanowire Synthesis and Its Application in a Highly Transparent, Conductive and Flexible Metal Electrode Touch Panel. *Nanoscale* **2012**, *4* (20), 6408−6414.
(29) Ran, Y.; He, W.; Wang, K.; Ji, S.; Ye, C. A One-Step Route to Ag Nanowires with a Diameter Below 40 Nm and an Aspect Ratio above 1000. *Chem. Commun.* **2014**, *50* (94), 14877−14880.

DOI: 10.1021/acsami.5b06489
ACS Appl. Mater. Interfaces 2015, 7, 21652−21656